
Scalable Privacy-enhanced Benchmark Graph Generative Model for Graph Convolutional Networks

Minji Yoon
Carnegie Mellon University

Yue Wu
Carnegie Mellon University

John Palowitch
Google Research

Bryan Perozzi
Google Research

Ruslan Salakhutdinov
Carnegie Mellon University

Abstract

A surge of interest in Graph Convolutional Networks (GCN) has produced thousands of GCN variants, with hundreds introduced every year. In contrast, many GCN models re-use only a handful of benchmark datasets as many graphs of interest, such as social or commercial networks, are proprietary. We propose a new graph generation problem to enable generating a diverse set of benchmark graphs for GCNs following the distribution of a source graph — possibly proprietary — with three requirements: 1) benchmark effectiveness as a substitute for the source graph for GCN research, 2) scalability to process large-scale real-world graphs, and 3) a privacy guarantee for end-users. With a novel graph encoding scheme, we reframe large-scale graph generation problem into medium-length sequence generation problem and apply the strong generation power of the Transformer architecture to the graph domain. Extensive experiments across a vast body of graph generative models show that our model can successfully generate benchmark graphs with the realistic graph structure, node attributes, and node labels required to benchmark GCNs on node classification tasks.

1 Introduction

Graph convolutional networks (GCNs) are machine learning models that generalize differentiable convolution operations, initially developed for image classification, to data objects with an arbitrary graph structure, from molecules to social networks Kipf and Welling (2016a). Various GCN models break ground across a wide variety of domain-specific tasks that use graphs as their natural data structure, including misinformation detection Benamira et al. (2019), drug discovery Xiong et al. (2019), traffic prediction Zhao et al. (2019), and social recommendation Ying et al. (2018).

GCN architectural innovations are usually evaluated on a handful of datasets from a small set of domains, such as citation networks (e.g., Cora, Citeseer, Pubmed Shchur et al. (2018)) or molecule graphs Hu et al. (2020)). This scarcity of benchmarks is known to incentivize researchers to develop new GCNs that are biased to optimize performance only on these benchmarks rather than generalize well (Palowitch et al., 2022), which is a known phenomenon in computer vision Yang et al. (2020). These observations harken to the fact that the standard datasets for benchmarking graph learning models come from domains that are easy to label, such as academic citation networks, rather than domains of priority interest to graph learning practitioners, such as social networks and real-world physical networks. Indeed, such networks are overwhelmingly proprietary and privacy-restricted and thus almost always unavailable for researchers to study or evaluate new GCN architectures.

In this paper, we propose to overcome the unavailability of critical real-world graph datasets with *graph generative models*. While there is already a vast body of work studying graph generation, even for producing differentially-private graph datasets Qin et al. (2017); Proserpio et al. (2012),

we found that no one study has addressed all necessary aspects of the modern-day setting, where large-scale graphs with node attributes/labels are necessary for responsible and impactful GCN research. Specifically, we propose the following novel graph generation problem definition:

Problem Definition 1. When $\mathcal{A} \in \mathbb{R}^{n \times n}$, $\mathcal{X} \in \mathbb{R}^{n \times d}$, and $\mathcal{Y} \in \mathbb{R}^n$ denote adjacency, node attribute, and node label matrices, respectively, given an original graph $\mathcal{G} = (\mathcal{A}, \mathcal{X}, \mathcal{Y})$, we generate a synthetic graph $\mathcal{G}' = (\mathcal{A}', \mathcal{X}', \mathcal{Y}')$ that satisfies following three requirements:

- **Benchmark effectiveness:** performance rankings among m GCN models on \mathcal{G}' should be similar to the rankings among the same m GCN models on \mathcal{G} .
- **Scalability:** time complexity of synthetic graph generation should be linearly proportional to the size of the original graph $O(|\mathcal{G}|)$.
- **Privacy guarantee:** any syntactic privacy notions are given to end users (e.g., k -anonymity or differential privacy).

In this paper we introduce the Computation Graph Transformer (CGT) as the core of a graph generation approach with two novel components that together solve the problem above. First, CGT operates on *training-time minibatches* rather than the graph as a whole, eliminating scalability problems encountered with nearly all existing generative models for graphs. We point out that each minibatch is in fact a GCN *computation graph* Hamilton et al. (2017) composed of its own adjacency and feature submatrices, and the set of all minibatches comprise a graph minibatch distribution that can be learned by an appropriate generative model.

Second, instead of attempting to learn the joint distribution of adjacency matrices and feature matrices, we derive a novel *duplicate encoding* scheme that transforms a (A, X) adjacency matrix, feature matrix pair into a single, dense feature matrix that is isomorphic to the original pair. In this way we are able to reduce the task of learning graph distributions to learning feature vector sequence distributions, which we approach with a novel transformer architecture Vaswani et al. (2017). This reduction is the key innovation allowing CGT to be an effective generator of realistic GCN training datasets. In addition, during the reduction process, our model can be easily extended to provide k -anonymity or differential privacy guarantees on node attributes and edge distributions.

To show the effectiveness of CGT, we design three experiments that examine its scalability, its effectiveness as a dataset generator for GCN training, and its privacy-performance trade-off. Specifically, to check its effectiveness as a dataset generator, we perturb various aspects of the GCN models and datasets, and check that these perturbations have the same empirical effect on GCN performance on both the CGT graphs and the original graphs. In total, our contributions are:

- **Modern problem statement for graph generation:** We propose a novel graph generation problem featuring three requirements for efficacy in state-of-the-art graph learning settings.
- **Minibatch distribution learning:** We reframe the problem of learning a distribution of a whole graph into learning the distribution of minibatches that are consumed by GCN models during training on large-scale datasets.
- **Transformer for graph generation:** We propose the Computation Graph Transformer (CGT), an architecture that casts the problem of computation graph generation as conditional sequence modeling.
- **Extensive experiments:** To check the benchmark effectiveness of graph generative models, we run 9 different GCN models on 7 real-world graphs with 16 different scenarios.

2 Related Work

While the study of graph generative models is a broad and active subfield, most approaches for attributed graphs target small-scale molecule/protein graphs with distinct attribute specs, and hence are not scalable to modern application settings, nor generalizable to other diverse domains. On the other hand, many generative models have been developed for non-attributed graphs, but these cannot be used for GCN research, given the lack of node features and labels. In this section we detail some of this existing work.

Traditional generative models extract the common patterns among the real-world graphs (e.g. nodes/edge/triangle counts, degree distribution, graph diameter, clustering coefficient) Chakrabarti and Faloutsos (2006) and generate new graphs following a few heuristic rules Erdős et al. (1960); Leskovec et al. (2010); Leskovec and Faloutsos (2007); Albert and Barabási (2002). However, they cannot learn unseen patterns from new graphs You et al. (2018). More importantly, they generate only graph structures, sometimes with low-dimensional boolean node attributes Eswaran et al. (2018).

General-purpose deep generative models exploit GAN Goodfellow et al. (2014), VAE Kingma and Welling (2013), and RNN Zaremba et al. (2014) architectures to learn graph distributions Guo and Zhao (2020). Most of them focus on learning graph structures You et al. (2018); Liao et al. (2019); Simonovsky and Komodakis (2018); Grover et al. (2019). Their evaluation metrics are graph statistics such as orbit counts, degree coefficients, and clustering coefficients which do not consider quality of generated node attributes and labels.

Molecule graph generative models are actively studied for generating promising candidate molecules using VAE Jin et al. (2018), GAN De Cao and Kipf (2018), RNN Popova et al. (2019), and recently invertible flow models Shi et al. (2020); Luo et al. (2021). However, most of their architectures are specialized to small scaled molecule graphs (e.g., 38 nodes per graph in the ZINC datasets) with low-dimensional attribute space (e.g., 9 boolean node attribute indicating atom types) and distinct molecule-related information (e.g., SMILES representation or chemical structures such as bonds and rings) Suhail et al. (2021).

Privacy-enhanced graph synthesis has been studied to ensure differentially-private (DP) Dwork (2008) graph generation Friedman and Schuster (2010). However, these approaches are limited to small-scaled graphs using few heuristic rules with no node attributes Qin et al. (2017); Proserpio et al. (2012). Some GCN models have been proposed with DP guarantees Olatunji et al. (2021); Sajadmanesh and Gatica-Perez (2021), but this line of work concerns the *models* and not the *training data*, and is therefore outside of our scope.

3 Reframing of graph generation problem into sequence generation problem

To develop a scalable and privacy-enhanced benchmark graph generative model for GCNs, we first look into how GCNs process a given graph \mathcal{G} which is commonly given as a pair of the adjacency matrix and node attribute matrix $(\mathcal{A}, \mathcal{X})$. Then, with two consecutive reframings of the problem, we convert our problem, learning distributions of a single graph, into a problem of learning distributions of sequences of discrete values.

3.1 Importance of computation graphs

Early implementations of GCN models execute convolutions on the whole adjacency matrix and node attribute matrix simultaneously Kipf and Welling (2016a), computing all node embeddings at every mini-batch. As the size of graph datasets grew, and GCN architectures evolved to contain neighborhood sampling schemes Hamilton et al. (2017), GCN training implementations relied on subgraph computation at each minibatch. Specifically, for each target node in the minibatch, L -layered GCNs first subsample a **computation graph** that is composed of nodes within L hops from the target node. Since L -layer GCNs cannot reach beyond L hops, this implementation does not affect the learned model at all, while allowing GCNs to scale to billion-node graphs by maintaining complexity proportional to the size of the minibatch subgraphs.

A computation graph \mathcal{G}_v of node v can be represented, equivalently to the global graph, by a sub-adjacency matrix $\mathcal{A}_v \in \mathbb{R}^{n_v \times n_v}$ and a sub-feature matrix $\mathcal{X}_v \in \mathbb{R}^{n_v \times d}$ where each with n_v rows corresponding to the nodes sampled into the computation graph. Additionally, each computation graph \mathcal{G}_v has a label $\mathcal{Y}_v \in \mathbb{R}$ of the target node. With our observation that modern GCNs train on minibatch computation graphs, our problem can be reduced to: *given a set of computation graphs, $\{\mathcal{G}_v = (\mathcal{A}_v, \mathcal{X}_v, \mathcal{Y}_v) : v \in \mathcal{G}\}$, we generate a set of computation graphs $\{\mathcal{G}'_v = (\mathcal{A}'_v, \mathcal{X}'_v, \mathcal{Y}'_v)\}$.* This reframing shares intuition with mini-batch stochastic gradient descent that the distribution of randomly chosen subsets approximates the distribution of the original set Bottou (2010).

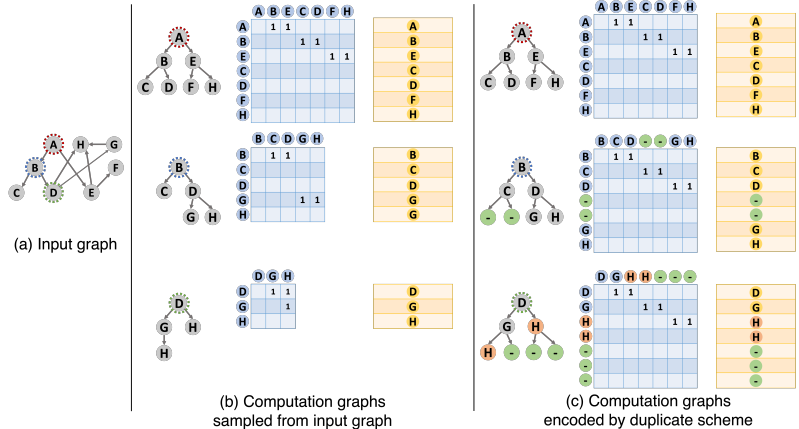


Figure 1: Encoding scheme for 2-layered computation graphs with sampling number 2: (a) input graph, (b) original encoding scheme outputs different shapes of adjacency matrices and node attribute matrices for each computation graph, (c) duplicate encoding scheme outputs the same adjacency matrix and the same shape of node attribute matrices.

3.2 Encoding scheme for computation graphs

We briefly explain how to generate a computation graph using the neighbor sampling scheme described in GraphSage Hamilton et al. (2017). In L -layered GCN, a computation graph is generated in a top-down manner ($l : L \rightarrow 1$) with the sampling number s . A target node v is located at the L -th layer; the target node samples s neighbors, and the sampled s nodes are located at the $(L - 1)$ -th layer; each node samples s neighbors, and the sampled s^2 nodes are located at the $(L - 2)$ -th layer; repeat until the 1-st layer. When a node has fewer neighbors than the sampling number s , we just sample all existing neighbors of the node. When we set the sampling number as the maximum degree in the graph, the computation graph-based GCN computation is the same with the computation using the whole graph.

The way to generate a computation graph is similar to generate a balanced s -nary tree structure (a balanced binary tree-shaped computation graph for node A in Figure 1(b)). However, in practice, computation graphs are barely in the balanced s -nary tree shape because of two cases: 1) lack of neighbors, and 2) neighbor sharing. In Figure 1(b), node C has fewer neighbors than the sampling number 2, thus the computation graphs for nodes B fail to maintain the binary tree shape. In the node D 's computation graph, nodes D and G share node H and make a cycle, thus the computation graph fails to maintain tree shape. As shown in Figure 1(b), this two cases result in the variable shapes of adjacency matrices (blue) and node attribute matrices (orange) of computation graphs.

3.3 Duplicate encoding scheme for computation graphs

We introduce a duplicate encoding scheme for computation graphs that is conceptually simple but brings a significant consequence: it allows us to *fix the adjacency matrix for all computation graphs* and treat it as a constant that does not need to be learned. For the first case breaking the s -nary tree structure of computation graphs, the *lack of neighbors*, the duplicate encoding scheme defines a null node with zero attribute vector (node $-$ in Figure 1(c)) and samples it as a padding neighbor for every node with less than s neighbors. For the *neighbor sharing among nodes in the computation graph* case, the duplicate encoding scheme duplicates shared neighbors and provides each copy to parent nodes (node H in node D 's computation graph in Figure 1(c)). Each node attribute vector is also duplicated and added to the feature matrix. As shown in Figure 1(c), with the duplicate encoding scheme, all computation graphs now have the same adjacency matrix presenting the s -nary balanced tree structure and the same *shape* of feature matrices. In order to fix the adjacency matrix, we fix the order of nodes in adjacency and attribute matrices (e.g., breadth-first ordering in Figure 1(c)). If all computation graphs have the same adjacency matrix, our problem of learning distributions over computation graphs becomes learning distributions of only feature matrices of computation graphs. We can formalize this new problem statement as: *given a set of feature matrix-label pairs $\{(\tilde{\mathcal{X}}_v, \mathcal{Y}_v) : v \in \mathcal{G}\}$ of computation graphs encoded with the duplicate scheme, we generate a set of feature matrix-label pairs $\{(\tilde{\mathcal{X}}'_v, \mathcal{Y}'_v)\}$.*

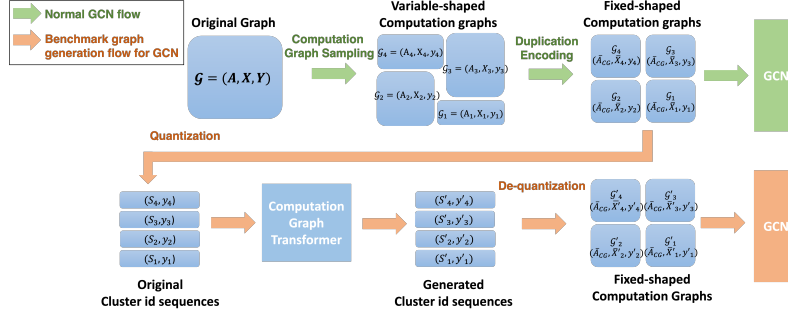


Figure 2: Overview of our benchmark graph generation framework.

3.4 Quantization

Next, we turn our attention to learning distributions of feature matrices, or in other words, feature vector sequences in computation graphs. We quantize feature vectors into discrete bins; specifically, we cluster feature vectors in the original graph into k clusters using k -means and map each feature vector to its (discrete) cluster id. This is a modeling decision independent of our problem formulation, motivated by 1) privacy benefits and 2) ease of modeling. By quantizing feature vectors into cluster centers, we can easily guarantee privacy for node attributes and edge distributions (more details in Section 4.2). Additionally, by reducing context from high dimensional feature vectors to discrete cluster ids, we can leverage Transformer state-of-the-art sequence generative models Vaswani et al. (2017); Chen et al. (2020). Finally, we reduced our problem to *learning distributions over sequences of discrete values — sequences of cluster ids of feature vectors in each computation graph*. At inference time, after the Transformer generates a new sequence of cluster ids, we replace each cluster id with the mean of the original feature vectors belonging to the cluster.

3.5 End-to-end framework for a benchmark graph generation problem

Figure 2 summarizes the entire process of mapping a graph generation problem into a discrete sequence generation problem. In the training phase, we 1) sample a set of (computation graph, label) pairs from the input graph, 2) encode each computation graph using the duplicate encoding scheme to fix adjacency matrices, 3) cluster feature vectors in the original graph and map each feature vector to the id of the cluster it belongs to, and finally 4) hand over a set of (sequence of cluster ids, label) pairs to our new Transformer architecture to learn their distribution. In the generation phase, we follow the same process in the opposite direction: 1) the trained Transformer outputs a set of (sequence of cluster ids, label) pairs, 2) we map cluster ids back into the feature vector space by replacing them with the average feature vector of the cluster, 3) we produce a computation graph from each sequence of feature vectors by reversing the duplicate encoding scheme, and 4) we feed the set of (computation graph, label) pairs to the GCN model we want to train or evaluate.

4 Model

We present the Computation Graph Transformer (CGT) that casts computation graph generation as conditional sequence modeling with minimal modification to the transformer architecture Vaswani et al. (2017). Then we check our model satisfies the three requirements — benchmark effectiveness, privacy, and scalability — from Problem Definition 1.

4.1 Computation Graph Transformer

Transformers consist of stacked self-attention layers with residual connections to efficiently model sequence data Vaswani et al. (2017). In this work, we extend a two-stream self-attention mechanism, XLNet Yang et al. (2019), which modifies the transformer architecture with a causal self-attention mask to enable auto-regressive generation. Given a sequence $s = [s_1, \dots, s_T]$, the L -layered

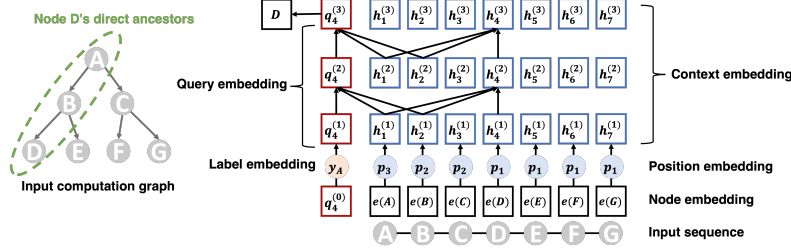


Figure 3: Computation Graph Transformer

transformer maximizes the likelihood under the forward auto-regressive factorization as follow:

$$\max_{\theta} \log p_{\theta}(\mathbf{s}) = \sum_{t=1}^T \log p_{\theta}(s_t | \mathbf{s}_{<t}) = \sum_{t=1}^T \log \frac{\exp(q_{\theta}^{(L)}(\mathbf{s}_{1:t})^{\top} e(s_t))}{\sum_{s'} \exp(q_{\theta}^{(L)}(\mathbf{s}_{1:t})^{\top} e(s'))}$$

where node embedding $e(s_t)$ maps discrete input id s_t to a randomly initialized trainable vector, and query embedding $q_{\theta}(\mathbf{s}_{1:t})$ encodes context information until t -th token in the sequence. More details on the Transformer architecture can be found in the Appendix. Here we describe how we modify the Transformer structure to model our computation graph effectively.

Position embeddings: In the original architecture, each token receives a position embedding p_t to let the Transformer recognize the token’s position in the sequence. In our model, however, sequences are flattened computation graphs (input sequence in Figure 3). To encode the original computation graph structure, we give different position embeddings to different layers in the computation graph while nodes at the same layer share the same position embedding. In Figure 3, node D, E, F and G located at the 1-st layer in the computation graph have the same position embedding p_1 .

Attention Masks: In the original architecture, query and context embeddings, $q_t^{(l)}$ and $h_t^{(l)}$, attend to all context embeddings $\mathbf{h}_{1:t-1}^{(l)}$ before t . In the computation graph, each node is sampled based on its parent node (which is sampled based on its own parent nodes) and is not directly affected by its sibling nodes. To encode this relationship more effectively, we mask all nodes except direct ancestor nodes in the computation graph, i.e., the target node (root) and any nodes between the target node and the leaf node. In Figure 3, node D ’s context/query embeddings attend only to direct ancestors, nodes A and B .

Label conditioning: In graphs, neighbor node distributions are not only affected by each node’s feature information but also by their label. It is well-known that GCNs improve over MLP performance by adding the convolutional operations that augment each node’s features with neighboring node features. This improvement is commonly attributed to nodes whose feature vectors are noisy (outliers among nodes with the same label) but that are connected with "good" neighbors (whose features are well-aligned with the label). In this case, without label information, we cannot learn whether a node has feature-wise homogeneous neighbors or feature-wise heterogeneous neighbors with the same labels. In our Transformer model, query embeddings $q_t^{(0)}$ are initialized with label embeddings that encode the label of each node into randomly initialized trainable vectors.

4.2 Theoretical analysis

We show our framework for benchmark graph generation can be easily extended to satisfy the two requirements, privacy and scalability, mentioned in the Problem Definition 1. First, we can provide k -anonymity for node attributes and edge distributions by using k -means clustering algorithm Bradley et al. (2000) with the minimum cluster size k during the quantization phase.

Claim 1 (k -Anonymity for node attributes). *In the generated computation graphs, each node attribute and edge distribution appear at least k times, respectively.*

During quantization, each node id is replaced with the id of the node’s cluster, reducing the original $(n \times n)$ graph into a $(m \times m)$ hypergraph where $m = n/k$. In the hypergraph, there are at most m different node attributes and m different edge distributions. During the de-quantization phase, a

Table 1: GCN performance varying number of noisy edges (#NE)

#NE	Model	Cora		Citeseer		Pubmed		AmazonP	
		Original	Generated	Original	Generated	Original	Generated	Original	Generated
0	GCN	0.85±0.010	0.84±0.068	0.71±0.001	0.49±0.028	0.85±0.006	0.62±0.001	0.90±0.001	0.84±0.035
	SGC	0.85±0.006	0.83±0.059	0.71±0.007	0.50±0.042	0.85±0.001	0.63±0.057	0.90±0.001	0.83±0.042
	GIN	0.84±0.005	0.80±0.042	0.70±0.001	0.52±0.049	0.81±0.007	0.63±0.028	0.89±0.002	0.83±0.035
	GAT	0.84±0.015	0.79±0.024	0.72±0.002	0.48±0.007	0.84±0.006	0.63±0.057	0.89±0.007	0.84±0.032
2	GCN	0.76±0.013	0.54±0.086	0.55±0.007	0.35±0.014	0.71±0.001	0.42±0.021	0.88±0.001	0.68±0.035
	SGC	0.74±0.003	0.54±0.080	0.54±0.006	0.34±0.013	0.71±0.005	0.43±0.014	0.86±0.006	0.66±0.007
	GIN	0.75±0.004	0.53±0.071	0.55±0.001	0.35±0.021	0.71±0.007	0.43±0.007	0.87±0.008	0.62±0.001
	GAT	0.71±0.021	0.48±0.075	0.51±0.035	0.35±0.014	0.75±0.002	0.43±0.035	0.85±0.006	0.67±0.042
4	GCN	0.69±0.007	0.43±0.019	0.49±0.008	0.28±0.071	0.64±0.003	0.47±0.028	0.85±0.007	0.60±0.007
	SGC	0.68±0.012	0.44±0.010	0.45±0.003	0.27±0.028	0.65±0.007	0.48±0.042	0.82±0.010	0.59±0.030
	GIN	0.69±0.015	0.46±0.027	0.50±0.007	0.25±0.025	0.65±0.014	0.46±0.014	0.83±0.008	0.56±0.024
	GAT	0.62±0.022	0.36±0.033	0.44±0.010	0.28±0.057	0.69±0.005	0.48±0.028	0.82±0.007	0.59±0.021
Pearson		0.978		0.965		0.824		0.908	
Spearman		0.972		0.835		0.469		0.926	

$(m \times m)$ hypergraph is mapped back to a $(n \times n)$ graph by letting k nodes in each cluster follow their cluster’s node attributes/edge distributions. Then, all k nodes belonging to the same cluster will have the same node attribute and edge distributions. Thus each node attribute and edge distribution appear at least k times in a generated graph.

Next, we can provide differential privacy (DP) for node attributes and edge distributions by exploiting DP k-means clustering algorithm Chang et al. (2021) during the quantization phase and DP stochastic gradient descent (DP-SGD) Song et al. (2013) to train the transformer. Unfortunately, however, DP-SGD for transformer is not well developed yet practically. So we can not guarantee the *rigid* differential privacy for edge distributions in practice (experimental results in Section 5.4). Thus, here, we only claim how DP k-means obscures node attributes inside of each cluster. We explain how we can guarantee differential privacy for edge distributions theoretically with ideal DP-SGD in Appendix.

Claim 2 ((ϵ, δ) -Differential Privacy for node attributes). *With probability at least $1 - \delta$, our generative model A gives ϵ -differential privacy for any graph \mathcal{G} , any node $v \in \mathcal{G}$, and any new computation graph \mathcal{G}_c generated from our model as follows:*

$$e^{-\epsilon} \leq \frac{\Pr[A(\mathcal{G}) = \mathcal{G}_c]}{\Pr[A(\mathcal{G}_{-v}) = \mathcal{G}_c]} \leq e^{\epsilon}$$

Claim 3 (Scalability). *When we aim to generate L -layered computation graphs with sampling number s on a graph with n nodes, computational complexity of our model is $O(s^{2L}n + k^2)$ where k is the number of nodes participating in the k -means computation.*

The full proofs for Claim 1, 2, 3 can be found in Appendix.

5 Experiments

To evaluate the benchmark effectiveness requirement, we focus on the node classification task, one of the most popular tasks on proprietary graphs.

5.1 Experimental setting

Dataset: we use six public datasets — three citation networks (Cora, Citeseer, and Pubmed) Sen et al. (2008), two co-purchase graphs (Amazon Photo and Amazon Computer) Shchur et al. (2018), and one co-authorship graph (MS CoauthorCS) [21] Shchur et al. (2018). Results on other datasets can be found in the Appendix. **Metric:** Our goal is the generation of synthetic graphs where GCN models show similar performance as they do on the original graphs. To measure performance similarity, we run popular GCN architectures on a pair of original and synthetic graphs, then measure Pearson and Spearman correlations Myers et al. (2013) between GCN accuracies on each type of graph.

5.2 Scalability

To the best of our knowledge, no other generic graph generative model was designed to output all of the adjacency matrix, node attribute matrix, and node labels. We extend three VAE-based

Table 2: Sampling-based GCN performance varying number of noisy edges (#NE)

#NE	Model	Cora		Citeseer		Pubmed		AmazonP	
		Original	Generated	Original	Generated	Original	Generated	Original	Generated
0	GraphSage	0.73±0.005	0.57±0.070	0.67±0.008	0.45±0.056	0.76±0.014	0.45±0.014	0.73±0.014	0.51±0.057
	ASGCN	0.34±0.005	0.27±0.036	0.24±0.003	0.19±0.024	0.32±0.049	0.31±0.099	0.38±0.021	0.41±0.057
	FastGCN	0.55±0.023	0.49±0.045	0.44±0.007	0.34±0.025	0.64±0.106	0.52±0.092	0.88±0.014	0.79±0.051
	PASS	0.76±0.003	0.59±0.062	0.66±0.014	0.43±0.032	0.76±0.007	0.44±0.035	0.80±0.007	0.49±0.028
2	GraphSage	0.29±0.008	0.17±0.025	0.27±0.016	0.22±0.018	0.45±0.007	0.34±0.007	0.49±0.014	0.39±0.085
	ASGCN	0.31±0.010	0.21±0.004	0.23±0.006	0.17±0.020	0.33±0.085	0.35±0.071	0.35±0.035	0.23±0.028
	FastGCN	0.34±0.012	0.26±0.014	0.24±0.001	0.22±0.021	0.45±0.099	0.42±0.078	0.82±0.007	0.73±0.025
	PASS	0.60±0.007	0.30±0.029	0.51±0.020	0.26±0.006	0.75±0.007	0.35±0.014	0.77±0.001	0.44±0.059
4	GraphSage	0.12±0.004	0.11±0.023	0.21±0.011	0.17±0.017	0.33±0.004	0.31±0.004	0.38±0.014	0.32±0.071
	ASGCN	0.28±0.012	0.17±0.014	0.20±0.002	0.14±0.006	0.47±0.007	0.40±0.021	0.27±0.019	0.23±0.028
	FastGCN	0.24±0.013	0.22±0.015	0.19±0.002	0.17±0.007	0.47±0.003	0.41±0.004	0.78±0.010	0.79±0.064
	PASS	0.48±0.066	0.18±0.057	0.44±0.015	0.20±0.012	0.74±0.001	0.30±0.001	0.75±0.007	0.44±0.007
Pearson		0.886		0.914		0.403		0.825	
Spearman		0.863		0.929		0.543		0.907	

Table 3: Sampling-based GCN performance on generated graphs varying sampling number (#SN)

#SN	Model	Cora		Citeseer		Pubmed		AmazonP	
		Original	Generated	Original	Generated	Original	Generated	Original	Generated
0	GCN	0.77±0.004	0.54±0.036	0.67±0.014	0.45±0.072	0.75±0.009	0.38±0.061	0.82±0.007	0.59±0.014
	SGC	0.74±0.004	0.48±0.023	0.66±0.016	0.42±0.056	0.76±0.002	0.38±0.045	0.73±0.001	0.53±0.028
	GIN	0.34±0.002	0.23±0.014	0.25±0.016	0.21±0.021	0.31±0.017	0.34±0.020	0.30±0.092	0.22±0.035
	GAT	0.57±0.021	0.40±0.014	0.45±0.003	0.32±0.063	0.55±0.009	0.40±0.052	0.69±0.255	0.60±0.191
2	GCN	0.82±0.015	0.67±0.039	0.68±0.008	0.52±0.079	0.78±0.004	0.54±0.049	0.89±0.007	0.66±0.053
	SGC	0.82±0.012	0.68±0.036	0.69±0.010	0.51±0.070	0.80±0.004	0.54±0.041	0.84±0.006	0.68±0.057
	GIN	0.34±0.006	0.26±0.006	0.25±0.010	0.19±0.031	0.27±0.007	0.31±0.002	0.27±0.071	0.25±0.035
	GAT	0.78±0.011	0.59±0.043	0.59±0.007	0.49±0.048	0.75±0.002	0.61±0.001	0.83±0.078	0.76±0.031
4	GCN	0.80±0.015	0.65±0.038	0.68±0.003	0.57±0.119	0.80±0.007	0.68±0.009	0.90±0.007	0.74±0.007
	SGC	0.83±0.003	0.69±0.042	0.70±0.007	0.59±0.14	0.82±0.001	0.71±0.043	0.87±0.014	0.79±0.021
	GIN	0.33±0.025	0.22±0.034	0.24±0.011	0.20±0.029	0.27±0.021	0.23±0.080	0.34±0.219	0.22±0.071
	GAT	0.78±0.009	0.62±0.017	0.59±0.004	0.56±0.129	0.74±0.014	0.65±0.043	0.86±0.014	0.81±0.021
Pearson		0.974		0.937		0.659		0.962	
Spearman		0.995		0.840		0.590		0.804	

graph generative models, GVAE Kipf and Welling (2016b), Graph VAE Simonovsky and Komodakis (2018), and Graphite Grover et al. (2019) to generate node attributes and labels in addition to adjacency matrices from their latent variables. We also choose three molecule graph generative models, GraphAF Shi et al. (2020), GraphDF Luo et al. (2021), and GraphEBM Suhail et al. (2021), that do not rely on any molecule-specific traits (e.g., SMILES representation).

GraphAF, GraphDF, and Graphite meet out-of-memory errors on even the smallest dataset, Cora. This is not surprising, given they were originally designed for small-size molecule graphs. The remaining baselines (GVAE, Graph VAE, and GraphEBM), however, fail to learn any meaningful node attribute/label distributions from the original graphs. For instance, the predicted distribution sometimes collapses to generating the the same node feature/labels across all nodes, which is obviously not the most effective benchmark (100% accuracy for all GCN models). We show their results and our analysis in the Appendix. Only our method can successfully generate benchmark graphs across all datasets with meaningful node attribute/label distributions (Tables 1, 2 and 3).

5.3 Benchmark effectiveness

To examine the benchmark effectiveness of our model, we design 4 different experiment environments where the performance of different GCN architectures varies widely. In each experiment environment,

Table 4: Privacy-Performance trade-off in benchmark graph generation

#NE	Model	Org	Base	K-anonymity			DP kmean (delta = 0.01)			DP SGD	
				K=100	k=500	k=1000	e = 1	e = 10	e = 25	e = 10 ⁻⁶	e = 10 ⁻⁹
0	GCN	0.85	0.84	0.77	0.49	0.12	0.45	0.57	0.65	0.13	0.64
	SGC	0.85	0.83	0.77	0.49	0.12	0.43	0.59	0.62	0.15	0.62
	GIN	0.84	0.8	0.74	0.51	0.11	0.48	0.57	0.65	0.14	0.64
	GAT	0.84	0.79	0.73	0.5	0.08	0.44	0.56	0.64	0.14	0.61
2	GCN	0.76	0.54	0.57	0.38	0.11	0.35	0.4	0.45	0.11	0.58
	SGC	0.74	0.54	0.58	0.36	0.08	0.35	0.41	0.45	0.14	0.57
	GIN	0.75	0.53	0.59	0.39	0.14	0.39	0.41	0.47	0.14	0.58
	GAT	0.71	0.48	0.56	0.38	0.11	0.35	0.39	0.43	0.12	0.53
4	GCN	0.69	0.43	0.51	0.28	0.09	0.28	0.39	0.43	0.1	0.41
	SGC	0.68	0.44	0.5	0.28	0.11	0.3	0.41	0.45	0.14	0.41
	GIN	0.69	0.46	0.48	0.3	0.16	0.32	0.41	0.46	0.15	0.4
	GAT	0.62	0.36	0.47	0.29	0.08	0.25	0.37	0.45	0.14	0.38
Pearson		1.000	0.978	0.972	0.955	0.081	0.960	0.916	0.885	0.182	0.919

we provide 3 variations and run 4 GCN models. Descriptions of each GCN model can be found in the Appendix. We measure Pearson and Spearman correlation coefficients of the GCN performance across all variations in each dataset.

Effects of noisy edges on aggregation strategies. We choose four different GCN models with different aggregation strategies: GCN (Kipf and Welling, 2016a) with mean aggregator, GIN Xu et al. (2018) with sum aggregator, SGC Wu et al. (2019) with linear aggregator, and GAT Veličković et al. (2017) with attention aggregator. Then we add noisy edges (randomly connected with any node in the graph) to each node and check how the GCN performance changes. In Table 1, when noisy edges are added, the accuracy across all GCN models drops in the original graphs. These trends can be nearly exactly captured in GCN performance on the generated graphs (both Pearson and Spearman correlation rates are up to 0.978). This shows that the synthetic graphs generated by our method successfully capture the noisy edge distributions introduced in the original graphs.

Effects of noisy edges on neighbor sampling. We choose four different GCN models with different neighbor sampling strategies: GraphSage Hamilton et al. (2017) with random sampling, FastGCN Chen et al. (2018) with heuristic layer-wise sampling, AS-GCN Huang et al. (2018) with trainable layer-wise sampling, and PASS Yoon et al. (2021) with trainable node-wise sampling. We then add noisy edges as described in the previous experiment and check how the different sampling policies deal with noisy neighbors. Table 2 shows that, similarly to the previous experiment, as noisy edges are added, the performance of all GCN architectures drops simultaneously across original graphs and generated graphs. PASS, the sampling policy with the best robustness to noisy edges, shows the highest accuracy when 2 or 4 edges are added per node on both the original and generated graphs on the Citeseer dataset. On the other hand, on the AmazonP dataset, FastGCN shows higher accuracy than PASS on the original graphs, and this trend is preserved on the generated graphs. This shows the strong benchmark effectiveness of our generative model. Researchers and practitioners can use graphs generated by our model to substitute original proprietary graphs while preserving the ranking of GCN architectures.

Effects of sampling number on neighbor sampling. We choose the same four GCN models with different neighbor sampling strategies as in the previous experiment. Then we change the number of sampled neighbor nodes and check how the GCN performance is affected. As more neighbors are sampled, GCN performance generally increases on the original graphs. This trend is successfully captured in the generated graphs with up to 0.995% Spearman correlation coefficient.

Effects of distribution shift. This experiment is based on the biased training set sampler proposed in Zhu et al. (2021) to examine each GCN model’s robustness to distribution shift in the training/test time. The biased sampler picks a few seed nodes and finds nearby nodes using the Personalized PageRank (PPR) vectors $\pi_{\text{ppr}}(I - (1 - \alpha)\tilde{A})^{-1}$, then uses them to compose a biased training set. We choose four different GCN models: GCN, SGC, GAT, and PPNP, as the authors of the original paper Zhu et al. (2021) chose for their baselines. We vary α and check how each GCN models deal with the biased training set. In Table 5 (in Appendix), surprisingly, the performance of GCN models drops at the beginning with $\alpha = 0.01$, then jump back with higher $\alpha = 0.3$. The generated graphs successfully capture these trends. This shows that our graph generative model is able to learn distribution shifts between training and test sets by learning from only computation graphs appearing in the training/test sets individually.

5.4 Privacy

We examine the performance-privacy trade-off across different privacy guarantees. For the k -anonymity, we use the k -means clustering algorithm Bradley et al. (2000) varying the minimum cluster size k . For differential privacy for node attributes, we use DP k -means Chang et al. (2021) varying the the sensitivity ϵ while setting $\delta = 0.01$. As expected, higher k and smaller ϵ (stronger privacy) hinder the generative model’s ability to learn the exact distributions of the original graphs, and the performance gap of GCN models between original and generated graphs increases (lower Pearson coefficient). For differential privacy for edge distributions, we use DP stochastic gradient descent Song et al. (2013) to train the transformer, varying the the sensitivity ϵ while setting $\delta = 0.1$. As shown in Table 4, even with astronomical $\epsilon = e^6$, the performance of our generative model degrades significantly. When we set $\epsilon = e^9$, we can finally see a reasonable performance. This shows the limited performance of DP SGD on the transformer architecture.

6 Conclusion

We propose a new graph generation problem to enable generating a diverse set of benchmark graphs for GCNs following the distribution of a source graph with three requirements: 1) benchmark effectiveness, 2) privacy guarantee, and 3) scalability. With a novel graph encoding scheme, we reframe a large-scale graph generation problem into a medium-length sequence generation problem and apply the strong generation power of the Transformer architecture to the graph domain. Our model successfully generates benchmark graphs following distributions of a diverse set of real-world graphs and shows the generated graphs can be used as substitutes for proprietary graphs to evaluate GCN innovations.

Limitation of the study: This paper shows that clustering-based solutions can achieve k-anonymity privacy guarantees. We stress, however, that implementing a real-world system with strong privacy guarantees will need to consider many other aspects beyond the scope of this paper. We leave as future work the study of whether we can combine stronger privacy guarantees with those of k-anonymity to enhance privacy protection.

References

- Réka Albert and Albert-László Barabási. 2002. Statistical mechanics of complex networks. *Reviews of modern physics* 74, 1 (2002), 47.
- Adrien Benamira, Benjamin Devillers, Etienne Lesot, Ayush K Ray, Manal Saadi, and Fragkiskos D Malliaros. 2019. Semi-supervised learning and graph neural networks for fake news detection. In *2019 IEEE/ACM International Conference on Advances in Social Networks Analysis and Mining (ASONAM)*. IEEE, 568–569.
- Léon Bottou. 2010. Large-scale machine learning with stochastic gradient descent. In *Proceedings of COMPSTAT'2010*. Springer, 177–186.
- Paul S Bradley, Kristin P Bennett, and Ayhan Demiriz. 2000. Constrained k-means clustering. *Microsoft Research, Redmond* 20, 0 (2000), 0.
- Deepayan Chakrabarti and Christos Faloutsos. 2006. Graph mining: Laws, generators, and algorithms. *ACM computing surveys (CSUR)* 38, 1 (2006), 2–es.
- Alisa Chang, Badih Ghazi, Ravi Kumar, and Pasin Manurangsi. 2021. Locally private k-means in one round. In *International Conference on Machine Learning*. PMLR, 1441–1451.
- Jie Chen, Tengfei Ma, and Cao Xiao. 2018. Fastgcn: fast learning with graph convolutional networks via importance sampling. *arXiv preprint arXiv:1801.10247* (2018).
- Mark Chen, Alec Radford, Rewon Child, Jeffrey Wu, Heewoo Jun, David Luan, and Ilya Sutskever. 2020. Generative pretraining from pixels. In *International Conference on Machine Learning*. PMLR, 1691–1703.
- Nicola De Cao and Thomas Kipf. 2018. MolGAN: An implicit generative model for small molecular graphs. *arXiv preprint arXiv:1805.11973* (2018).
- Cynthia Dwork. 2008. Differential privacy: A survey of results. In *International conference on theory and applications of models of computation*. Springer, 1–19.
- Paul Erdős, Alfréd Rényi, et al. 1960. On the evolution of random graphs. *Publ. Math. Inst. Hung. Acad. Sci* 5, 1 (1960), 17–60.
- Dhivya Eswaran, Reihaneh Rabbany, Artur W Dubrawski, and Christos Faloutsos. 2018. Social-affiliation networks: Patterns and the SOAR model. In *Joint European conference on machine learning and knowledge discovery in databases*. Springer, 105–121.
- Arik Friedman and Assaf Schuster. 2010. Data mining with differential privacy. In *Proceedings of the 16th ACM SIGKDD international conference on Knowledge discovery and data mining*. 493–502.

- Ian Goodfellow, Jean Pouget-Abadie, Mehdi Mirza, Bing Xu, David Warde-Farley, Sherjil Ozair, Aaron Courville, and Yoshua Bengio. 2014. Generative adversarial nets. *Advances in neural information processing systems* 27 (2014).
- Aditya Grover, Aaron Zweig, and Stefano Ermon. 2019. Graphite: Iterative generative modeling of graphs. In *International conference on machine learning*. PMLR, 2434–2444.
- Xiaojie Guo and Liang Zhao. 2020. A systematic survey on deep generative models for graph generation. *arXiv preprint arXiv:2007.06686* (2020).
- Will Hamilton, Zitao Ying, and Jure Leskovec. 2017. Inductive representation learning on large graphs. *Advances in neural information processing systems* 30 (2017).
- Weihua Hu, Matthias Fey, Marinka Zitnik, Yuxiao Dong, Hongyu Ren, Bowen Liu, Michele Catasta, and Jure Leskovec. 2020. Open graph benchmark: Datasets for machine learning on graphs. *Advances in neural information processing systems* 33 (2020), 22118–22133.
- Wenbing Huang, Tong Zhang, Yu Rong, and Junzhou Huang. 2018. Adaptive sampling towards fast graph representation learning. *Advances in neural information processing systems* 31 (2018).
- Wengong Jin, Regina Barzilay, and Tommi Jaakkola. 2018. Junction tree variational autoencoder for molecular graph generation. In *International conference on machine learning*. PMLR, 2323–2332.
- Diederik P Kingma and Max Welling. 2013. Auto-encoding variational bayes. *arXiv preprint arXiv:1312.6114* (2013).
- Thomas N Kipf and Max Welling. 2016a. Semi-supervised classification with graph convolutional networks. *arXiv preprint arXiv:1609.02907* (2016).
- Thomas N Kipf and Max Welling. 2016b. Variational graph auto-encoders. *arXiv preprint arXiv:1611.07308* (2016).
- Johannes Klicpera, Aleksandar Bojchevski, and Stephan Günnemann. 2018. Predict then propagate: Graph neural networks meet personalized pagerank. *arXiv preprint arXiv:1810.05997* (2018).
- Jure Leskovec, Deepayan Chakrabarti, Jon Kleinberg, Christos Faloutsos, and Zoubin Ghahramani. 2010. Kronecker graphs: an approach to modeling networks. *Journal of Machine Learning Research* 11, 2 (2010).
- Jure Leskovec and Christos Faloutsos. 2007. Scalable modeling of real graphs using kronecker multiplication. In *Proceedings of the 24th international conference on Machine learning*. 497–504.
- Renjie Liao, Yujia Li, Yang Song, Shenlong Wang, Will Hamilton, David K Duvenaud, Raquel Urtasun, and Richard Zemel. 2019. Efficient graph generation with graph recurrent attention networks. *Advances in Neural Information Processing Systems* 32 (2019).
- Meng Liu, Youzhi Luo, Limei Wang, Yaochen Xie, Hao Yuan, Shurui Gui, Haiyang Yu, Zhao Xu, Jingtun Zhang, Yi Liu, et al. 2021. DIG: a turnkey library for diving into graph deep learning research. *Journal of Machine Learning Research* 22, 240 (2021), 1–9.
- Youzhi Luo, Keqiang Yan, and Shuiwang Ji. 2021. GraphDF: A discrete flow model for molecular graph generation. In *International Conference on Machine Learning*. PMLR, 7192–7203.
- Jerome L Myers, Arnold D Well, and Robert F Lorch Jr. 2013. *Research design and statistical analysis*. Routledge.
- Iyiola E Olatunji, Thorben Funke, and Megha Khosla. 2021. Releasing Graph Neural Networks with Differential Privacy Guarantees. *arXiv preprint arXiv:2109.08907* (2021).
- John Palowitch, Anton Tsitsulin, Brandon Mayer, and Bryan Perozzi. 2022. GraphWorld: Fake Graphs Bring Real Insights for GNNs. *arXiv preprint arXiv:2203.00112* (2022).

- Mariya Popova, Mykhailo Shvets, Junier Oliva, and Olexandr Isayev. 2019. MolecularRNN: Generating realistic molecular graphs with optimized properties. *arXiv preprint arXiv:1905.13372* (2019).
- Davide Proserpio, Sharon Goldberg, and Frank McSherry. 2012. A workflow for differentially-private graph synthesis. In *Proceedings of the 2012 ACM workshop on Workshop on online social networks*. 13–18.
- Zhan Qin, Ting Yu, Yin Yang, Issa Khalil, Xiaokui Xiao, and Kui Ren. 2017. Generating synthetic decentralized social graphs with local differential privacy. In *Proceedings of the 2017 ACM SIGSAC Conference on Computer and Communications Security*. 425–438.
- Sina Sajadmanesh and Daniel Gatica-Perez. 2021. Locally private graph neural networks. In *Proceedings of the 2021 ACM SIGSAC Conference on Computer and Communications Security*. 2130–2145.
- Prithviraj Sen, Galileo Namata, Mustafa Bilgic, Lise Getoor, Brian Galligher, and Tina Eliassi-Rad. 2008. Collective classification in network data. *AI magazine* 29, 3 (2008), 93–93.
- Oleksandr Shchur, Maximilian Mumme, Aleksandar Bojchevski, and Stephan Günnemann. 2018. Pitfalls of Graph Neural Network Evaluation. *Relational Representation Learning Workshop, NeurIPS 2018* (2018).
- Chence Shi, Minkai Xu, Zhaocheng Zhu, Weinan Zhang, Ming Zhang, and Jian Tang. 2020. Graphaf: a flow-based autoregressive model for molecular graph generation. *arXiv preprint arXiv:2001.09382* (2020).
- Martin Simonovsky and Nikos Komodakis. 2018. Graphvae: Towards generation of small graphs using variational autoencoders. In *International conference on artificial neural networks*. Springer, 412–422.
- Shuang Song, Kamalika Chaudhuri, and Anand D Sarwate. 2013. Stochastic gradient descent with differentially private updates. In *2013 IEEE Global Conference on Signal and Information Processing*. IEEE, 245–248.
- Mohammed Suhail, Abhay Mittal, Behjat Siddiquie, Chris Broaddus, Jayan Eledath, Gerard Medioni, and Leonid Sigal. 2021. Energy-based learning for scene graph generation. In *Proceedings of the IEEE/CVF Conference on Computer Vision and Pattern Recognition*. 13936–13945.
- Ashish Vaswani, Noam Shazeer, Niki Parmar, Jakob Uszkoreit, Llion Jones, Aidan N Gomez, Łukasz Kaiser, and Illia Polosukhin. 2017. Attention is all you need. *Advances in neural information processing systems* 30 (2017).
- Petar Veličković, Guillem Cucurull, Arantxa Casanova, Adriana Romero, Pietro Lio, and Yoshua Bengio. 2017. Graph attention networks. *arXiv preprint arXiv:1710.10903* (2017).
- Felix Wu, Amauri Souza, Tianyi Zhang, Christopher Fifty, Tao Yu, and Kilian Weinberger. 2019. Simplifying graph convolutional networks. In *International conference on machine learning*. PMLR, 6861–6871.
- Zhaoping Xiong, Dingyan Wang, Xiaohong Liu, Feisheng Zhong, Xiaozhe Wan, Xutong Li, Zhaojun Li, Xiaomin Luo, Kaixian Chen, Hualiang Jiang, et al. 2019. Pushing the boundaries of molecular representation for drug discovery with the graph attention mechanism. *Journal of medicinal chemistry* 63, 16 (2019), 8749–8760.
- Keyulu Xu, Weihua Hu, Jure Leskovec, and Stefanie Jegelka. 2018. How powerful are graph neural networks? *arXiv preprint arXiv:1810.00826* (2018).
- Kaiyu Yang, Klint Qinami, Li Fei-Fei, Jia Deng, and Olga Russakovsky. 2020. Towards fairer datasets: Filtering and balancing the distribution of the people subtree in the imagenet hierarchy. In *Proceedings of the 2020 Conference on Fairness, Accountability, and Transparency*. 547–558.
- Zhilin Yang, Zihang Dai, Yiming Yang, Jaime Carbonell, Russ R Salakhutdinov, and Quoc V Le. 2019. Xlnet: Generalized autoregressive pretraining for language understanding. *Advances in neural information processing systems* 32 (2019).

- Rex Ying, Ruining He, Kaifeng Chen, Pong Eksombatchai, William L Hamilton, and Jure Leskovec. 2018. Graph convolutional neural networks for web-scale recommender systems. In *Proceedings of the 24th ACM SIGKDD international conference on knowledge discovery & data mining*. 974–983.
- Minji Yoon, Théophile Gervet, Baoxu Shi, Sufeng Niu, Qi He, and Jaewon Yang. 2021. Performance-Adaptive Sampling Strategy Towards Fast and Accurate Graph Neural Networks. In *Proceedings of the 27th ACM SIGKDD Conference on Knowledge Discovery & Data Mining*. 2046–2056.
- Jiaxuan You, Rex Ying, Xiang Ren, William Hamilton, and Jure Leskovec. 2018. Graphrnn: Generating realistic graphs with deep auto-regressive models. In *International conference on machine learning*. PMLR, 5708–5717.
- Wojciech Zaremba, Ilya Sutskever, and Oriol Vinyals. 2014. Recurrent neural network regularization. *arXiv preprint arXiv:1409.2329* (2014).
- Ling Zhao, Yujiao Song, Chao Zhang, Yu Liu, Pu Wang, Tao Lin, Min Deng, and Haifeng Li. 2019. T-gcn: A temporal graph convolutional network for traffic prediction. *IEEE Transactions on Intelligent Transportation Systems* 21, 9 (2019), 3848–3858.
- Qi Zhu, Natalia Ponomareva, Jiawei Han, and Bryan Perozzi. 2021. Shift-robust gnns: Overcoming the limitations of localized graph training data. *Advances in Neural Information Processing Systems* 34 (2021).

A Appendix

A.1 Architecture of Computation Graph Transformer

Given a sequence $\mathbf{s} = [s_1, \dots, s_T]$, the L -layered transformer maximizes the likelihood under the forward auto-regressive factorization as follow:

$$\max_{\theta} \log p_{\theta}(\mathbf{s}) = \sum_{t=1}^T \log p_{\theta}(s_t | \mathbf{s}_{<t}) = \sum_{t=1}^T \log \frac{\exp(q_{\theta}^{(L)}(\mathbf{s}_{1:t})^{\top} e(s_t))}{\sum_{s'} \exp(q_{\theta}^{(L)}(\mathbf{s}_{1:t})^{\top} e(s'))}$$

where node embedding $e(s_t)$ maps discrete input id s_t to a randomly initialized trainable vector, and query embedding $q_{\theta}(\mathbf{s}_{1:t})$ encodes context information until t -th token in the sequence. $q_{\theta}^{(l+1)}(\mathbf{s}_{1:t})$ is computed with context embeddings $\mathbf{h}_{1:t-1}^{(l)}$ of previous $t - 1$ tokens and query embedding $q_t^{(l)}$ from the previous layer. Context embedding $h_t^{(l)}$ is computed from $\mathbf{h}_{1:t}^{(l-1)}$, context embeddings of previous $t - 1$ tokens and t -th token from the previous layer. Note that, while the query embeddings have access only to the previous context embeddings $\mathbf{h}_{1:t-1}^{(l)}$, while the context embeddings attend to all tokens $\mathbf{h}_{1:t}^{(l)}$. The context embedding $h_t^{(0)}$ is initially encoded by node embeddings $e(s_t)$ and position embedding p_t that encodes the location of each token in the sequence. The query embedding is initialized with a trainable vector. This two streams (query and context) of self-attention layers are stacked L time and predict the next tokens auto-regressively.

A.2 Proof of Privacy Claims

Claim 4 (k -Anonymity for node attributes and edge distributions). *In the generated computation graphs, each node attribute and edge distribution appear at least k times, respectively.*

Proof. In the quantization phase, we use k-means clustering algorithm Bradley et al. (2000) with the minimum cluster size k . Then each node id is replaced with a cluster id the node belongs to, reducing the original $(n \times n)$ graph into a $(m \times m)$ hypergraph where $m = n/k$ is the number of clusters. Then Computation Graph Transformer learns edge distributions among m hyper nodes (i.e., clusters) and generates a new $(m \times m)$ hypergraph. In the hypergraph, there are at most m different node attributes and m different edge distributions. During the de-quantization phase, a $(m \times m)$ hypergraph is mapped back to a $(n \times n)$ graph by letting k nodes in each cluster follow their cluster's node attributes/edge distributions as follow: k nodes in the same cluster will have the same feature vector that is the average feature vector of original nodes belonging to the cluster. When s denotes the number of sampled neighbor nodes, each node samples s clusters (with replacement) following its cluster's edge distributions among m clusters. When a node samples cluster i , it will be connected to one of nodes in the cluster i randomly. At the end, each node will have s neighbor nodes randomly sampled from s clusters the node samples with the cluster's edge distribution, respectively. Likewise, all k nodes belonging to the same cluster will sample neighbors following the same edge distributions. Thus each k node attribute and edge distribution appear at least k times in a generated graph. ■

Claim 5 (ϵ, δ) -Differential Privacy for node attributes). *With probability at least $1 - \delta$, our generative model A gives ϵ -differential privacy for any graph \mathcal{G} , any node $v \in \mathcal{G}$, and any new computation graph \mathcal{G}_c generated from our model as follows:*

$$e^{-\epsilon} \leq \frac{\Pr[A(\mathcal{G}) = \mathcal{G}_c]}{\Pr[A(\mathcal{G}_{-v}) = \mathcal{G}_c]} \leq e^{\epsilon}$$

Proof. \mathcal{G}_{-v} denotes neighboring graphs to the original one \mathcal{G} , but without a specific node v . During the quantization phase, we use (ϵ, δ) -differential private k-means clustering algorithm on node features Chang et al. (2021). Then clustering results are differential private with regard to each node features. In the generated graphs, each node feature is decided by the clustering results (i.e., the average feature vector of nodes belonging to the same cluster). Then, by looking at the generated node features, one cannot tell whether any individual node feature was included in the original dataset or not. ■

Table 5: GCN performance on graphs generated by baseline generative models. Except our method, no existing graph generative models can generate a set of adjacency matrix, node feature matrix, and node label matrix that reproduce reasonable GCN performance.

Dataset	Model	Original	GraphAF	GraphDF	GraphEBM	Graphite	GVAE	Ours
Cora	GCN	0.850	o.o.m	o.o.m	1.000	o.o.m	0.2	0.840
	SGC	0.850	o.o.m	o.o.m	1.000	o.o.m	0.200	0.830
	GIN	0.840	o.o.m	o.o.m	1.000	o.o.m	0.200	0.800
	GAT	0.840	o.o.m	o.o.m	1.000	o.o.m	0.380	0.790
Citeseer	GCN	0.710	o.o.m	o.o.m	1.000	o.o.m	0.19	0.490
	SGC	0.705	o.o.m	o.o.m	1.000	o.o.m	0.180	0.500
	GIN	0.700	o.o.m	o.o.m	1.000	o.o.m	0.190	0.515
	GAT	0.720	o.o.m	o.o.m	1.000	o.o.m	0.380	0.475
Pearson correlation		1.000	-	-	-	-	0.090	0.989

Remark 1 ((ϵ, δ) -Differential Privacy for edge distributions). In our model, individual nodes’ edge distributions are learned and generated by the transformer. When we use (ϵ, δ) -differential private stochastic gradient descent (DP-SGD) Song et al. (2013) to train the transformer, the transformer becomes differentially private in the sense that by looking at the output (generated edge distributions), one cannot tell whether any individual node’s edge distribution (input to the transformer) was included in the original dataset or not. If we have DP-SGD that can train transformers successfully with reasonably small ϵ and δ , we can guarantee (ϵ, δ) -differential privacy for edge distribution of any graph generated by our generative model. However, as we show in Section 5.4, current DP-SGD is not stable yet for transformer training, leading to very coarse or impractical privacy guarantees.

Claim 6 (Scalability). *When we aim to generate L -layered computation graphs with sampling number s on a graph with n nodes, computational complexity of our model is $O(s^{2L}n + k^2)$ where k is the number of nodes participating in the k -means computation.*

Proof. During k -means, we randomly sample k node features to compute the cluster centers. Then we map each feature vector to the closest cluster center. By sampling k nodes, we limit the k -mean computation cost to $O(k^2)$. The sequence reduced from each computation graph is $O(1 + s + \dots + s^L)$ and the number of sequences (computation graphs) is $O(n)$. Then the training time of the transformer is proportional to $O(s^{2L}n)$. ■

A.3 Baselines

In Table 5, GraphAF, GraphDF, and Graphite meet out-of-memory errors on even the smallest dataset, Cora. This is not surprising, given they were originally designed for small-size molecule graphs. The remaining baselines (GVAE, Graph VAE, and GraphEBM), however, fail to learn any meaningful node attribute/label distributions from the original graphs. For instance, the predicted distribution sometimes collapses to generating the the same node feature/labels across all nodes, which is obviously not the most effective benchmark (100% accuracy for all GCN models on graphs generated by GraphEBM). This is because none of existing graph generative models is designed for GCN benchmarking — simultaneous generation of adjacency, node feature, and node label matrices, rather they all focus only on the generation of adjacency matrices. This result shows the tricky aspects of graph generation and relations among graph structure, node attributes and labels, and a large room for improvement for the graph generation field.

A.4 GCN models in Benchmark effectiveness

We choose four different GCN models with different aggregation strategies to examine the effect of noisy edges: GCN Kipf and Welling (2016a) with mean aggregator, GIN Xu et al. (2018) with sum aggregator, SGC Wu et al. (2019) with linear aggregator, and GAT Veličković et al. (2017) with attention aggregator. We choose four different GCN models with different neighbor sampling strategies: GraphSage Hamilton et al. (2017) with random sampling, FastGCN Chen et al. (2018) with heuristic layer-wise sampling, AS-GCN Huang et al. (2018) with trainable layer-wise sampling, and PASS Yoon et al. (2021) with trainable node-wise sampling. We choose four different GCN models: GCN Kipf and Welling (2016a), SGC Wu et al. (2019), GAT Veličković et al. (2017), and PPNP Klicpera et al. (2018), as the authors of the original paper Zhu et al. (2021) chose for their baselines.

Table 6: **GCN performance with distribution shift varying PPR coefficient (α)**. *Random* denotes no distribution shift between training and test datasets. Pearson and Spearman scores measure the correlation in ranking of GCN models on Original and Generated graphs; a score of 1 denotes perfect correlation.

α	Model	Cora		Citeseer		Pubmed		AmazonP	
		Original	Generated	Original	Generated	Original	Generated	Original	Generated
random	GCN	0.88±0.004	0.61±0.044	0.68±0.005	0.51±0.063	0.58±0.008	0.65±0.056	0.08±0.006	0.50±0.045
	SGC	0.55±0.011	0.44±0.031	0.59±0.031	0.31±0.071	0.5±0.022	0.54±0.034	0.60±0.009	0.58±0.052
	GAT	0.74±0.060	0.36±0.057	0.32±0.130	0.26±0.090	0.24±0.070	0.29±0.064	0.03±0.024	0.03±0.032
	PPNP	0.83±0.002	0.60±0.097	0.64±0.010	0.54±0.096	0.61±0.003	0.62±0.022	0.85±0.004	0.69±0.067
0.01	GCN	0.62±0.010	0.59±0.046	0.59±0.007	0.38±0.103	0.44±0.009	0.65±0.013	0.39±0.017	0.53±0.055
	SGC	0.13±0.069	0.13±0.150	0.47±0.013	0.29±0.054	0.64±0.053	0.71±0.088	0.05±0.038	0.46±0.008
	GAT	0.28±0.022	0.24±0.077	0.24±0.036	0.11±0.077	0.47±0.013	0.55±0.098	0.05±0.199	0.02±0.234
	PPNP	0.56±0.005	0.59±0.012	0.61±0.003	0.42±0.086	0.72±0.003	0.64±0.044	0.75±0.008	0.58±0.011
0.3	GCN	0.68±0.049	0.63±0.044	0.57±0.001	0.46±0.008	0.68±0.033	0.47±0.007	0.59±0.004	0.62±0.015
	SGC	0.46±0.222	0.30±0.074	0.51±0.002	0.19±0.034	0.71±0.045	0.45±0.045	0.06±0.233	0.52±0.089
	GAT	0.50±0.005	0.30±0.081	0.32±0.012	0.13±0.076	0.53±0.009	0.19±0.088	0.01±0.177	0.01±0.211
	PPNP	0.62±0.004	0.60±0.057	0.61±0.015	0.46±0.065	0.73±0.003	0.52±0.048	0.71±0.022	0.54±0.013
Pearson		0.807		0.872		0.362		0.717	
Spearman		0.842		0.907		0.042		0.926	

Table 7: **Effects of different aggregation strategies and neighbor sampling on Amazon Computer**. Pearson and Spearman scores measure the correlation in ranking of GCN models on Original and Generated graphs; a score of 1 denotes perfect correlation.

#NE	Model	Aggregation		#SN	Model	Sampling	
		Original	Generated			Original	Generated
0	GCN	0.84±0.005	0.57±0.015	1	GraphSage	0.73±0.004	0.20±0.023
	SGC	0.81±0.001	0.56±0.006		ASGCN	0.65±0.003	0.21±0.012
	GIN	0.81±0.012	0.53±0.002		FastGCN	0.37±0.008	0.35±0.009
	GAT	0.83±0.013	0.57±0.028		PASS	0.74±0.011	0.48±0.032
2	GCN	0.78±0.006	0.41±0.003	3	GraphSage	0.83±0.004	0.34±0.018
	SGC	0.75±0.010	0.36±0.021		ASGCN	0.78±0.008	0.43±0.008
	GIN	0.74±0.017	0.38±0.011		FastGCN	0.36±0.004	0.36±0.003
	GAT	0.79±0.002	0.42±0.008		PASS	0.76±0.013	0.51±0.020
4	GCN	0.77±0.006	0.38±0.027	5	GraphSage	0.77±0.017	0.45±0.029
	SGC	0.72±0.007	0.35±0.015		ASGCN	0.78±0.009	0.53±0.034
	GIN	0.74±0.019	0.33±0.005		FastGCN	0.36±0.006	0.35±0.004
	GAT	0.75±0.010	0.38±0.037		PASS	0.73±0.020	0.47±0.014
Pearson		0.939		Pearson		0.305	
Spearman		0.950		Spearman		0.357	

A.5 Effects of distribution shift in Section 5.3

Table 6 shows effects of distribution shift between training and test sets on GCN performance. We regulate the shift by controlling the Personalized PageRank coefficient α . The performance of GCN models drops at the beginning with $\alpha = 0.01$, then jump back with higher $\alpha = 0.3$. The generated graphs successfully capture these trends, by showing Pearson and Spearman correlation rates up to 0.872 and 0.926. This shows that our graph generative model is able to learn distribution shifts between training and test sets by learning from only computation graphs appearing in the training/test sets individually.

A.6 More results on other datasets

We use six public datasets — three citation networks (Cora, Citeseer, and Pubmed) Sen et al. (2008), two co-purchase graphs (Amazon Photo and Amazon Computer) Shchur et al. (2018), and one co-authorship graph (Microsoft CS) Shchur et al. (2018). Results on Amazon Computer and Microsoft CS can be found in the Tables 7 and 8.

A.7 Ablation study

To show the importance of each component in our Computation Graph Transformer, we run three ablation studies on our model. Table 9 shows CGT without label conditioning (conditioning on the label of the root node of the computation graph), positional embedding trick (giving the same positional embedding to nodes at the same layers on the computation graph), and masked attention trick (attended only on direct ancestor nodes on the computation graph), respectively. When we remove the positional embedding trick, we provide the different positional embeddings to all nodes in a computation graph, following the original transformer architecture. When we remove attention masks from our model, the transformer attends all other nodes in the computation graphs to compute

Table 8: Effects of different sampling strategies and distribution shift on Microsoft CS

#NE	Model	Sampling		α	Model	Shift	
		Original	Generated			Original	Generated
0	GraphSage	0.72±0.003	0.42±0.028	random	GCN	0.80±0.005	0.43±0.024
	ASGCN	0.21±0.022	0.22±0.071		SGC	0.59±0.017	0.39±0.001
	FastGCN	0.64±0.023	0.54±0.148		GAT	0.23±0.013	0.01±0.026
	PASS	0.80±0.001	0.41±0.007		PPNP	0.85±0.007	0.50±0.032
2	GraphSage	0.31±0.008	0.12±0.007	0.01	GCN	0.60±0.002	0.47±0.007
	ASGCN	0.07±0.110	0.12±0.004		SGC	0.54±0.023	0.44±0.004
	FastGCN	0.23±0.223	0.20±0.011		GAT	0.01±0.005	0.01±0.011
	PASS	0.77±0.005	0.10±0.005		PPNP	0.60±0.009	0.52±0.005
4	GraphSage	0.16±0.009	0.06±0.024	0.3	GCN	0.61±0.026	0.39±0.003
	ASGCN	0.15±0.155	0.13±0.001		SGC	0.61±0.025	0.45±0.021
	FastGCN	0.17±0.009	0.17±0.026		GAT	0.01±0.025	0.01±0.006
	PASS	0.73±0.005	0.06±0.032		PPNP	0.60±0.015	0.52±0.010
Pearson		0.470		Pearson		0.902	
Spearman		0.207		Spearman		0.573	

Table 9: Ablation study. Label, Position, and Attention denote ablation of label conditioning, positional embeddings, and masked attention proposed in Section 4.1, respectively. Pearson scores measure the correlation in ranking of GCN models on Original and Generated graphs; a score of 1 denotes perfect correlation.

Dataset	Model	Original	Label	Position	Attention	Ours
Cora	GCN	0.850	0.110	0.710	0.740	0.840
	SGC	0.850	0.130	0.690	0.740	0.830
	GIN	0.840	0.150	0.730	0.750	0.800
	GAT	0.840	0.120	0.710	0.740	0.790
Citeseer	GCN	0.710	0.190	0.560	0.480	0.490
	SGC	0.705	0.200	0.460	0.490	0.500
	GIN	0.700	0.180	0.540	0.490	0.515
	GAT	0.720	0.220	0.500	0.470	0.475
Pubmed	GCN	0.745	0.430	0.730	0.660	0.620
	SGC	0.745	0.360	0.720	0.670	0.630
	GIN	0.742	0.440	0.710	0.660	0.630
	GAT	0.745	0.570	0.730	0.610	0.630
Amazon Photo	GCN	0.900	0.150	0.780	0.770	0.835
	SGC	0.900	0.090	0.770	0.760	0.830
	GIN	0.885	0.100	0.760	0.770	0.825
	GAT	0.890	0.260	0.770	0.760	0.835
Pearson correlation		1.000	-0.517	0.751	0.903	0.961

the context embeddings. As shown in Table, removing any component negatively impacts model performance. This shows not only the importance of label conditioning and our designed positional embeddings and attention masks, but also tricky aspects of graph generation and relations among graph structure, node attributes and labels.

A.8 Experimental settings

All experiments were conducted on the same p3.2xlarge Amazon EC2 instance. We run each experiment three times and report the mean and standard deviation.

For the molecule graph generative models, GraphAF, GraphDF, and GraphEBM, we extend implementations in a public domain adaptation library DIG Liu et al. (2021). We extend implementations of GraphVAE¹, GVAE², Graphite³ from codes uploaded by authors. For our Computation Graph Transformer model, we use a transformer with 3 layers and 12 heads.

For GCN benchmark models, we implement GCN, SGC, GIN, and GAT from scratch for the aggregation strategy test. For the sampling strategy test, we use open source implementations of each GCN model, ASGCN⁴, FastGCN⁵, and PASS⁶, uploaded by original authors. Finally, for the distribution shift test, we use GCN, SGC, GAT, and PPNP implemented by Zhu et al. (2021) using DGL library⁷.

¹<https://github.com/JiaxuanYou/graph-generation/tree/master/baselines/graphvae>

²<https://github.com/tkipf/gae>

³<https://github.com/ermongroup/graphite>

⁴<https://github.com/huangwb/AS-GCN>

⁵<https://github.com/matenure/FastGCN>

⁶<https://github.com/linkedin/PASS-GNN>

⁷<https://github.com/GentleZhu/Shift-Robust-GNNs>

Table 10: **Dataset statistics.** AmazonC and AmazonP denote the Amazon Computer and Amazon Photo datasets, respectively. MS CS denotes the Microsoft Coauthor CS.

Dataset	Node	Edge	Feature	Label	Train/Val/Test
Cora	2,485	5,069	1,433	7	140/500/1,000
Citeseer	2,110	3,668	3,703	6	120/500/1,000
Pubmed	19,717	44,324	500	3	60/500/1,000
AmazonC	13,381	245,778	767	10	410/1,380/12,000
AmazonP	7,487	119,043	745	8	230/760/6,650
MS CS	18,333	81,894	6,805	15	550/1,830/15,950